PACS numbers: 42.55.Tv; 42.60.Da; 42.82.Et
DOI: 10.1070/QE2009v039n05ABEH013932

Mode selection in two-dimensional Bragg resonators based on planar dielectric waveguides

V.R. Baryshev, N.S. Ginzburg, V.Yu. Zaslavskii, A.M. Malkin, A.S. Sergeev, M. Thumm

***Abstract*. Two-dimensional Bragg resonators based on planar dielectric waveguides are analysed. It is shown that the doubly periodic corrugation deposited on the dielectric surface in the form of two gratings with translational vectors directed perpendicular to each other ensures effective selection of modes along two coordinates at large Fresnel parameters. This result is obtained both by the method of coupled waves (geometrical optics approximation) and by the direct numerical simulations. Two-dimensional Bragg resonators make it possible to fabricate two-dimensional distributed feedback lasers and to provide generation of spatially coherent radiation in large-volume active media.**

Keywords: *distributed feedback lasers, two-dimensional Bragg resonator, mode selection.*

1. Introduction

Conventional distributed feedback lasers [1–7] use the coupling of waveguide modes propagating in dielectric structures with aperiodic modulation of parameters, for example, the layer thickness:

$$b(z) = b_0 + b_1 \cos \bar{h} z, \tag{1}$$

where b_0 is the average layer thickness; b_1 is the modulation amplitude; $\bar{h} = 2\pi/d$; d is the modulation period. These structures produce a one-dimensional Bragg resonator in which two counterpropagating waves are scattered. This resonator provides efficient mode selection along their longitudinal index. In the case of the planar geometry, radiation mode-locking along the second transverse coordinate z can be ensured by the diffraction spread of wave beams if the transverse size l_x of the system is limited by the Fresnel condition $l_x^2/l_z\lambda < 1$, where l_z is the resonator length. Authors of paper [8] studied theoretically the efficient method of spatial mode-locking of radiation at large Fresnel parameters $l_x^2/l_z\lambda \gg 1$, which is based on the use of a two-dimensional distributed feedback. In the optical spectrum, a two-dimensional distributed feedback can be realised with the help of a dielectric plate with a doubly periodic sinusoidal modulation of one of the surfaces (Fig. 1a,b)

$$b(x,z) = b_0 + b_1[\cos \bar{h}(x+z) + \cos \bar{h}(x-z)] \tag{2}$$

with translational vectors $\boldsymbol{K}^{\pm} = \bar{h}\boldsymbol{x}_0 \pm \bar{h}\boldsymbol{z}_0$ directed perpendicular to each other ($\boldsymbol{x}_0$, $\boldsymbol{z}_0$ are the unit vectors of the coordinate system). Two-dimensional Bragg structure (2) provides coupling and mutual scattering of four partial wave fluxes $C_z^{\pm}$ and $C_x^{\pm}$ with wave vectors $\boldsymbol{h}$ propagating in $\pm z$ and $\pm x$ directions and specified by the vector potentials:

$$\boldsymbol{A} = \mathrm{Re}\Big\{\big[\boldsymbol{a}_1(y)\big(C_z^+ \mathrm{e}^{-\mathrm{i}hz} + C_z^- \mathrm{e}^{\mathrm{i}hz}\big) + \boldsymbol{a}_2(y)\big(C_x^+ \mathrm{e}^{-\mathrm{i}hz} + C_x^- \mathrm{e}^{\mathrm{i}hz}\big)\big]\mathrm{e}^{\mathrm{i}\omega t}\Big\}, \tag{3}$$

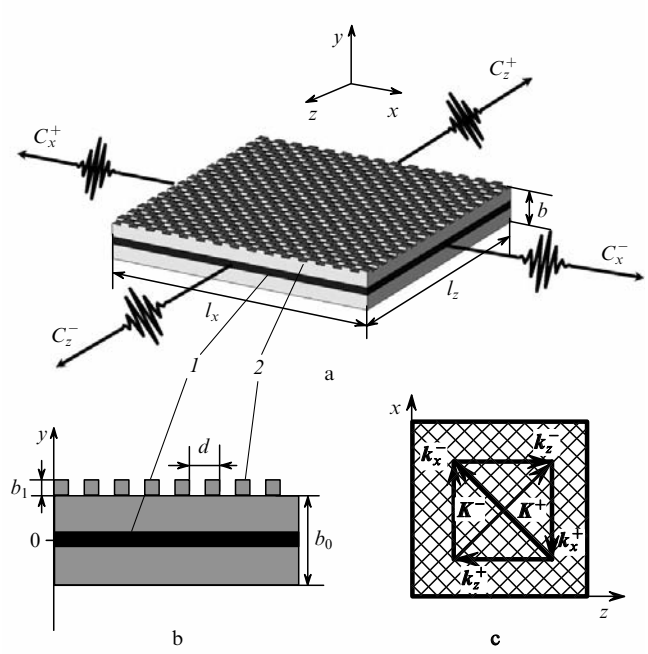

Figure 1. General scheme of a laser with a two-dimensional distributed feedback (a), transverse cross section of a two dimensional Bragg resonator (b) and the diagram illustrating scattering of partial waves (c); $\boldsymbol{k}_{x,z}^{\pm}$ are the wave vectors of partial waves; (*1*) active medium; (*2*) Bragg grating.

V.R. Baryshev, N.S. Ginzburg, V.Yu. Zaslavskii, A.M. Malkin, A.S. Sergeev Institute of Applied Physics, Russian Academy of Sciences, ul. Ul'yanova 46, 603950 Nizhnii Novgorod, Russia;
e-mail: baryshev@appl.sci-nnov.ru;
M. Thumm Forschungszentrum Karlsruhe, Association EURATOM-FZK, IHM, Hermann-von-Helmholtz Platz 1, D-76021 Karlsruhe, Germany

Received 17 June 2008; revision received 6 October 2008
Kvantovaya Elektronika **39** (5) 463–468 (2009)
Translated by I.A. Ulitkin

where $\boldsymbol{a}_{1,2}$ are transverse mode structures of a planar dielectric wavegude. Effective coupling of waves on structure (2) takes place when the resonance condition is fulfilled: $h \approx \bar{h}$ (see Fig. 1c). In this case, waves $C_z^{\pm}$ scatter into waves $C_x^{\pm}$, and the direct coupling of waves $C_z^- \leftrightarrow C_z^+$ and $C_x^- \leftrightarrow C_x^+$ is absent.

Note that similar to planar Bragg resonators of the microwave region, which are based on corrugated metal plates [9–11], the doubly periodic sinusoidal corrugation for practical realisations can be replaced by a chess-type corrugation (see Fig. 1a):

$$b(x,z) = b_0 + b_1 f(x) f(z),$$

$$f(\xi) = \begin{cases} 1, 2q\pi/\hbar < \xi < (2q+1)\pi/\hbar, \\ -1, (2q-1)\pi/\hbar < \xi < 2q\pi/\hbar, \ q = 1,2,\ldots \end{cases} \quad (4)$$

By using the method of coupled waves we studied selective properties of two-dimensional Bragg structures and showed that such systems ensure effective mode selection along two coordinates. In this case, the modes located in the vicinity of the Bragg frequency have the highest Q factor. These results are confirmed by the direct numerical simulation based on the standard CST Micro-Wave Studio code.

2. Eigenmodes of a two-dimensional Bragg structure

Eigenwaves of a planar dielectric waveguide are either TE- or TM-polarised. In the case of a one-dimensional Bragg structure, the waves of these polarisations are coupled [3]. For Bragg structure (2) studied below taking into account that the conditions for the Bragg scattering are fulfilled for partial waves C_x and C_z propagating in mutually perpendicular directions, only for the TM-polarised waves the partial waves have the common electric field component (E_y) and thus are efficiently coupled. For TE-polarised waves, the electric field is directed perpendicular to the wave vector and during scattering on structure (2) the electric fields of partial waves C_x and C_z are mutually perpendicular. Thus, the efficient coupling of waves with these polarisations is absent. Note, however, that it is possible to organise coupling of TE- and TM-polarised waves (C_x and C_z) but with a lower coupling coefficient than that in the case of TM-wave scattering. Let us restrict ourselves to the case when the width of the dielectric layer is associated with the condition $kb_0(\varepsilon - 1)^{1/2} < \pi$ (where $k = \omega_0/c$, ε is the dielectric constant) for which in the frequency range specified by the active medium band there is an only propagating TM-wave with one variation along the y axis (the number of variations is a quantity exceeding the number of field zeros by unity). The field components of partial waves can be presented in the form

$$a_{1y}(y) = a_{2y}(y) = \cos gy, \ a_{1z}(y) = a_{2x}(y) = \frac{-\mathrm{i}g}{h}\sin gy \quad (5)$$

for $|y| < l_y/2$,

$$a_{1y}(y) = a_{2y}(y) = \frac{g}{p}\sin\left(\frac{gl_y}{2}\right)\mathrm{e}^{-p|y|},$$

$$a_{1z}(y) = a_{2x}(y) = \frac{-\mathrm{i}g}{h}\sin\left(\frac{gl_y}{2}\right)\mathrm{e}^{-p|y|} \quad (6)$$

for $|y| > l_y/2$. Here, $g = (\varepsilon k^2 - h^2)^{1/2}$ and $p = (h^2 - k^2)^{1/2}$ are transverse wave numbers inside a dielectric and in vacuum, respectively, which can be found from the characteristic equation for symmetric TM-modes of a dielectric waveguide:

$$\left[(\varepsilon - 1)k^2 - g^2\right]^{1/2} = \frac{g}{\varepsilon}\tan\left(\frac{gl_y}{2}\right). \quad (7)$$

Mutual coupling and scattering of four partial wave fluxes on the two-dimensional Bragg structure in the geometric optics approximation, which is valid at large Fresnel numbers, is described by the system of equations [9]:

$$\frac{\partial C_z^{\pm}}{\partial z} \mp \mathrm{i}\delta C_z^{\pm} \pm \mathrm{i}\alpha(C_x^+ + C_x^-) = 0,$$

$$\frac{\partial C_x^{\pm}}{\partial x} \mp \mathrm{i}\delta C_x^{\pm} \pm \mathrm{i}\alpha(C_z^+ + C_z^-) = 0. \quad (8)$$

Here, $\delta = h(\omega_0) - \bar{h}$ is the frequency detuning from the frequency of the exact Bragg resonance and α is the coupling coefficient, which can be presented in the form [3]

$$\alpha = \frac{vb_1 h}{4}\frac{(\varepsilon - h^2/k^2)(1 + 1/\varepsilon^2)}{(h^2/\varepsilon^2 k^2 + h^2/k^2 - 1)b_0 + 2(h^2 - k^2)^{-1/2}}, \quad (9)$$

where $v = 1$ in the case of sinusoidal modulation (2) and $v = 16\pi^2$ in the case of chess corrugation (4).

By representing the solution of equations (8) in the form $\sim \mathrm{e}^{\mathrm{i}(\Lambda_x x + \Lambda_z z)}$, we obtain the dispersion equation for normal waves in the infinite two-dimensional Bragg structure:

$$(\delta^2 - \Lambda_x^2)(\delta^2 - \Lambda_z^2) - 4\alpha^2\delta^2 = 0. \quad (10)$$

At $\delta > 0$, dispersion characteristics $\delta(\Lambda_x, \Lambda_z)$ (Fig. 2) represent two sheets (at $\delta < 0$, the solution is mirror symmetric to that shown in the figure). Sheet (*1*) intersects the vertical axis at the point $\delta/\alpha = 2$ (mirror point $\delta/\alpha = -2$). These points correspond to the extrema of the function $\delta(\Lambda_x, \Lambda_z)$ at which the minima of the group velocities of normal waves are achieved. As shown below, a part of high-Q eigenmodes of the two-dimensional Bragg structure are located near these points. These modes, in principle, are similar to the modes of a conventional one-dimensional Bragg structure. The specific feature of the two-dimensional Bragg structure consists in the presence of

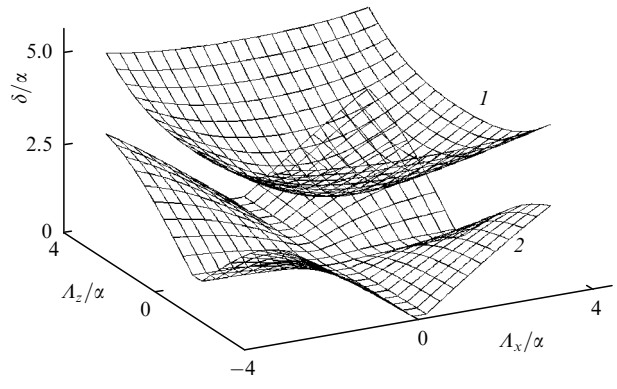

Figure 2. Dispersion parameters $\delta(\Lambda_x, \Lambda_z)$ of normal waves for the two-dimensional Bragg structure in the region $\delta > 0$.

sheet (*2*), which intersects the vertical axis at the point $\delta = 0$. For this sheet in the vicinity $\Lambda_{x,z} = 0$ not only the group velocity but also its derivatives tend to zero, which favours the formations of high-Q modes in the mentioned vicinity.

The spectrum of eignemodes can be found from the solution of Eqns (8) with boundary conditions

$$C_z^+\Big|_{z=0} = 0,\ C_z^-\Big|_{z=l_z} = 0,\ C_x^+\Big|_{x=0} = 0,\ C_x^-\Big|_{x=l} = 0, \quad (11)$$

at which external energy fluxes are absent.

To solve boundary problem (8), (11), we will introduce functions $F_z = C_z^+ + C_z^-$ and $F_x = C_x^+ + C_x^-$ for which equations (8) will be rewritten in the form

$$\frac{\partial^2 F_z}{\partial z^2} + \delta^2 F_z = -2\alpha\delta F_x,$$
$$\frac{\partial^2 F_x}{\partial x^2} + \delta^2 F_x = -2\alpha\delta F_z, \quad (12)$$

with boundary conditions

$$\left(\frac{\partial F_z}{\partial z} \mp \mathrm{i}\delta F_z\right)\Big|_{z=l_z/2\pm l_z/2} = 0,\ \left(\frac{\partial F_x}{\partial x} \mp \mathrm{i}\delta F_x\right)\Big|_{x=l_x/2\pm l_x/2} = 0. \quad (13)$$

Equations (12) can be solved by the method of separation of variables, by substituting expressions for $F_{x,z}$ in the form

$$F_z(x,z) = B_z f_x(x) f_z(z),$$
$$F_x(x,z) = B_x f_x(x) f_z(z), \quad (14)$$

where $B_{x,z}$ are arbitrary constants, $f_\xi(\xi)$ are the eigenfunctions of operators T_z and T_x;

$$T_\xi f(\xi) = \frac{\mathrm{d}^2 f(\xi)}{\mathrm{d}\xi^2} + \delta^2 f(\xi). \quad (15)$$

Eigenfunctions $f_\xi(\xi)$ of the operator T_ξ satisfying the equation $T_\xi f_\xi(\xi) = \gamma_\xi f_\xi(\xi)$ can be represented in the form

$$f_\xi(\xi) = \frac{(\delta + \Lambda_\xi)^{1/2}}{(\delta - \Lambda_\xi)^{1/2}}\Big\{(\delta + \Lambda_\xi)\exp\left[\mathrm{i}\Lambda_\xi(\xi + l_\xi/2)\right] - (\delta - \Lambda_\xi)\exp\left[-\mathrm{i}\Lambda_\xi(\xi - l_\xi/2)\right]\Big\}, \quad (16)$$

where $\Lambda_\xi = (\delta^2 - \gamma_\xi)^{1/2}$, γ_ξ is the eigenvalue of the operator T_ξ defined from the characteristic equation

$$\exp(2\mathrm{i}\Lambda_\xi l_\xi) = \frac{(\delta - \Lambda_\xi)^2}{(\delta + \Lambda_\xi)^2}. \quad (17)$$

By substituting (14) into expression (12), from the condition of the nontrivial solution condition we obtain the relation

$$\gamma_x\gamma_z = 4\alpha^2\delta^2. \quad (18)$$

Here, γ_x, γ_z are eigenvalues of the operators T_z and T_x, respectively. The solution of algebraic equation (18) determines the spectrum of complex resonator eigenfrequencies δ.

To determine the spatial field structures of partial waves constituting the resonator eigenmode, we will substitute (14) into (12) and after integration taking into account boundary conditions (13) we obtain:

$$C_z^\pm = 2\mathrm{i}\alpha(\delta \pm \Lambda_z)\exp(\pm\mathrm{i}\Lambda_z l_z/2)\sin[\Lambda_z(z \pm l_z/2)]f_x(x),$$
$$C_x^\pm = 2\mathrm{i}\alpha(\delta \pm \Lambda_x)\exp(\pm\mathrm{i}\Lambda_x l_x/2)\sin[\Lambda_x(x \pm l_x/2)]f_z(z). \quad (19)$$

Under conditions of strong coupling of waves $\alpha l_{x,z} \gg 1$, we can solve boundary problem (8), (11) in the explicit form [9]

$$\delta_{n,m} = \pm\frac{\pi^2 mn}{2\alpha l_z l_x} + \mathrm{i}\frac{\pi^2}{2\alpha^2 l_z l_x}\left(\frac{n^2}{l_z} + \frac{m^2}{l_x}\right), \quad (20a)$$

$$\delta_{n,m} = \pm\left[2\alpha + \frac{\pi^2}{4\alpha}\left(\frac{n^2}{l_z^2} + \frac{m^2}{l_x^2}\right)\right] + \mathrm{i}\frac{\pi^2}{2\alpha^2}\left(\frac{n^2}{l_z^3} + \frac{m^2}{l_x^3}\right), \quad (20b)$$

where n and m are the subscripts of modes along the longitudinal and transverse coordinates.

Frequencies and Q factors of eigenmodes are determined, respectively, by the real and imaginary parts of the eigenvalue $\delta_{n,m}$:

$$\omega_{n,m} \approx c\hbar + c\,\mathrm{Re}\,\delta_{n,m}, \quad (21a)$$

$$Q_{n,m} \approx (\bar{h}/2)\mathrm{Im}\,\delta_{n,m}. \quad (21b)$$

According to (20), the two-dimensional Bragg resonator has a high selectivity both in the longitudinal n and transverse m mode subscripts. This selectivity is ensured by the excitation of electromagnetic energy fluxes not only in the longitudinal direction ($\pm z$) (which takes place in conventional one-dimensional Bragg resonators [1–7]) but additionally in the transverse direction ($\pm x$). The resonator eigenmodes are located in the vicinity of the exact Bragg resonance frequency $\bar{\omega} = \bar{h}c$ [$\delta = 0$, (20a)] as well as in the vicinity of the Bragg scattering region $\delta \approx \pm 2\alpha$ (20b) (Fig. 3). It is obvious that the modes described by expression (20b) have analogues in the mode spectrum of a one-dimensional Bragg resonator and are associated with sheet (*1*) (see Fig. 2) of dispersion parameters of normal waves. A specific feature of two-dimensional Bragg resonators is the presence of high-Q modes located in the absence of corrugation defects in the centre of the Bragg band and described by expression (20a). These modes are associated with sheet (*2*) of dispersion parameters. Modes

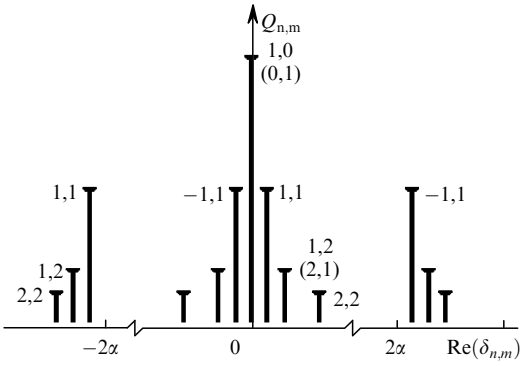

Figure 3. Mode spectrum of the two-dimensional Bragg resonator.

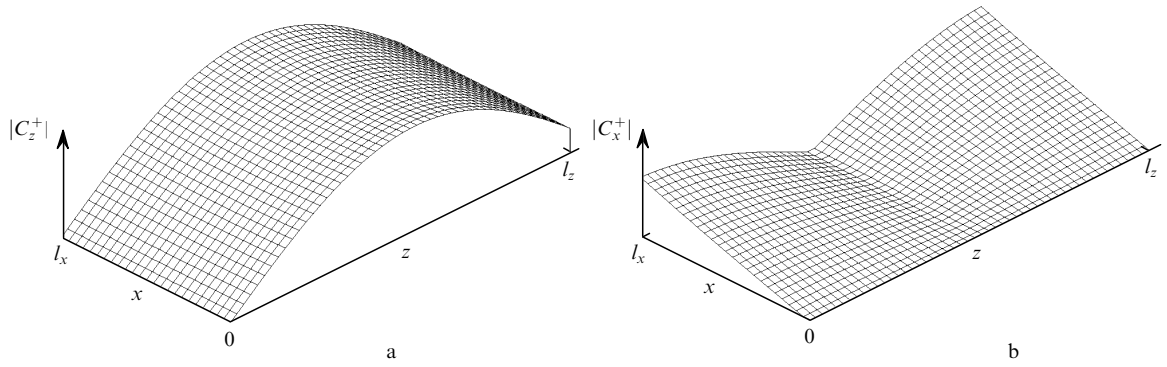

Figure 4. Field structure of partial waves C_z^+ (a) and C_x^+ (b) for the fundamental mode with the subscripts $\{n = 0, m = 1\}$; $l_z = 5$, $l_x = 2.5$.

with subscripts $\{n = 0, m = 1\}$ and $\{n = 1, m = 0\}$ have the highest Q factors (Fig. 3). These modes in the applied geometrical optics approximation are degenerate with respect to the frequency and in the case $l_x = l_z$ they are degenerate with respect to the Q factor. To remove the degeneracy with respect to the Q factor, it is necessary to use the rectangular structures. At $l_z > l_x$ the mode with the subscripts $\{n = 1, m = 0\}$ has the highest Q factor. According to (20, (21), the Q factor of this mode is determined by the relation

$$Q_{1,0} = \frac{\bar{h}k^2\alpha^2 l_z^2 l_x}{\pi^2}. \tag{22}$$

It should be emphasised that within the framework of the used assumptions (geometrical optics approximation and neglect of ohmic losses) the relation between the mode Q factors with different subscripts is independent of the geometric dimensions of the system. The field structures of partial waves of the fundamental mode for the case $l_z = 2l_x$ are presented in Fig. 4. To refine the value of the fundamental mode Q factor at relatively small parameters $\alpha l_{x,z}$, we solved equation (18) numerically by using the particle swarm optimisation (PSO) method. The results presented in Fig. 5 demonstrate that relation (22) yields good approximation for the Q factor at $\alpha l_z > 2$.

It is important to note that the existence of modes inside the Bragg resonance band in the absence of periodicity defects is a specific feature of the two-dimensional Bragg structures under study, which differ both from one-dimensional (one periodic) prototypes [1–4] and from two-dimensional photonic crystals [12–14], where periodicity defects should be introduced to produce modes.

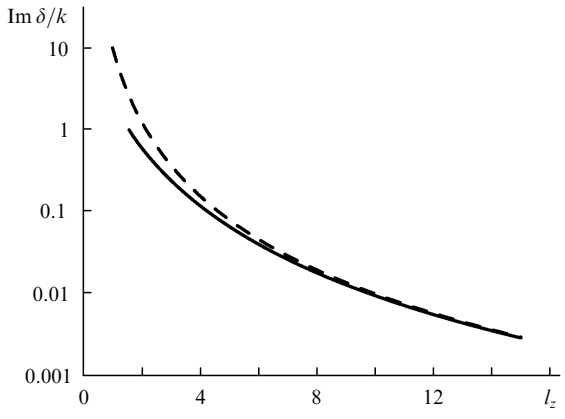

Figure 5. Dependence of δ for the fundamental mode on the resonator dimension at $l_x = l_z/2$; the dashed cure shows the analytic dependence in the approximation $\alpha l_{x,z} \gg 1$.

3. Simulation of selective parameters of two-dimensional Bragg structures

To confirm the results of the analytic consideration, we performed additional simulation of electrodynamic parameters of planar two-dimensional Bragg structures based on dielectric waveguides within the framework of a three-dimensional electromagnetic CST MicroWave Studio code. The eigenmodes of the electrodynamic system were determined by simulating its excitation by the external short current pulse from a point dipole placed inside the resonator. The duration of the 'powering' current pulse was $\omega_0\Delta t \approx 40$, which corresponded to the spectral width $\Delta\omega/\omega_0 \approx 0.3$. We analysed the field evolution inside the resonator. After several passes of partial wave fluxes in the resonator, characteristic maxima, which correspond to the position of the highest-Q eigenmodes, should be formed in the spectrum of the excited field.

Figures 6, 7 present the results of simulation for the resonator with the plate thickness $b_0 = 0.45\lambda$, dielectric constant $\varepsilon = 1.5$, width $l_x = 27\lambda$ and length $l_z = 81\lambda$ (the Fresnel parameters are $N_z = l_z^2/\lambda l_x \approx 250$ and $N_x = l_x^2/\lambda l_z \approx 10$). The corrugation depth was $b_1 = 0.045\lambda$ and the period was $d = 0.925\lambda$. The exciting dipole was placed at the point with the coordinates $(2l_x/3, 2l_z/3)$. The total simulation time was $\omega_0 t_{\max} \approx 8000$, which corresponds to $\sim 20 - 30$ passes of waves in the resonator.

The evolution of the electic field at some point inside the structure $E_y(l_x/3, l_z/3; t)$ at the entire simulation interval is shown in Fig. 6a. Figure 6b presents the exponential field decay at the interval $\omega_0 t \approx 3000 - 6000$ at which the fundamental mode is selected. For comparison, the same figure shows the curve corresponding to the signal decay with the decrement, which was obtained by solving characteristic equation (18) for the fundamental mode of the Bragg resonator. One can see good agreement between the simulation results and the results of analytic consideration within the framework of the method of coupled waves. The Q factor $Q_{1,0}$ calculated by the field decay velocity was ~ 500. Figure 6 also shows the signal spectrum calculated during the entire simulation time (Fig. 6c) and at the finite time interval (Fig. 6d). It follows from these figures that the

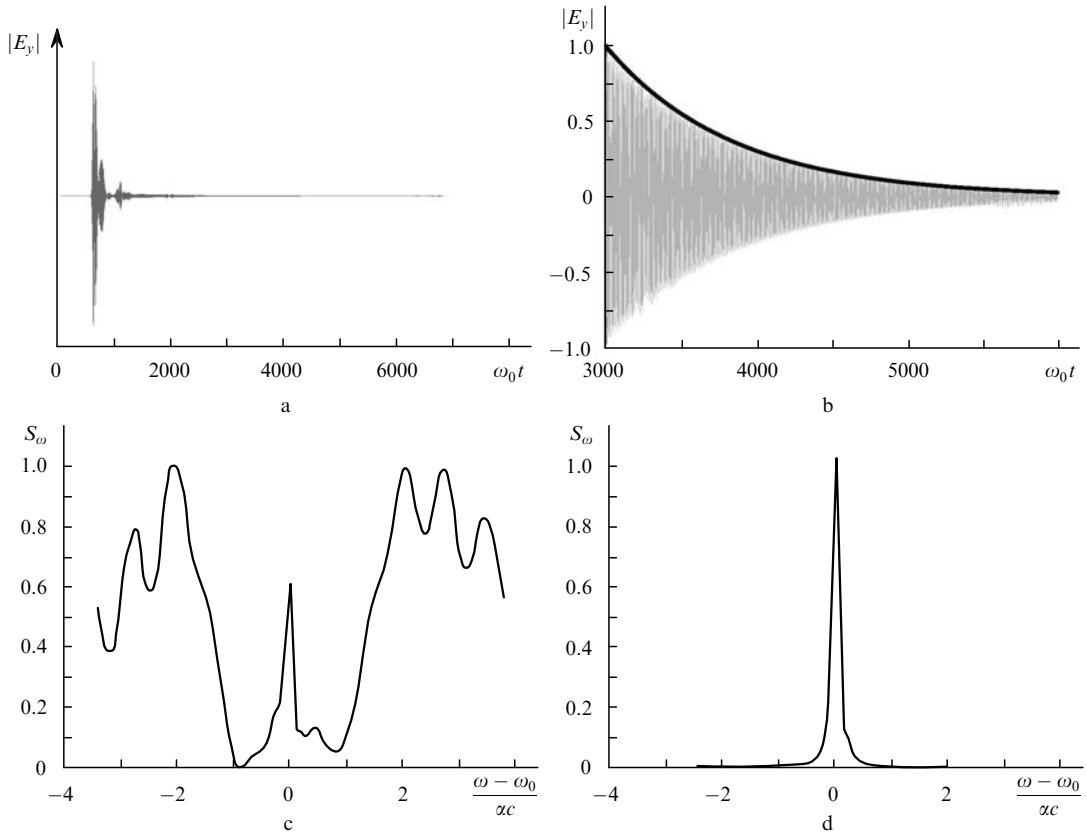

Figure 6. Simulation results of excitation of the two-dimensional structure by a short electromagnetic pulse: amplitude evolution of the field projection $|E_y|$ at the observation point over the entire simulation interval ($\omega_0 t \approx 0 - 8000$) (a), field evolution at the stage of the exponential decay ($\omega_0 t \approx 3000 - 6000$), for comparison thick curve shows the signal decay with the decrement obtained from the solution of characteristic equation (18) (b) as well as the field spectra S_ω (c) and (d) corresponding to (a) and (b), respectively; $l_z = 81\lambda$, $l_x = 27\lambda$, $b_0 = 0.45\lambda$, $\varepsilon = 1.5$.

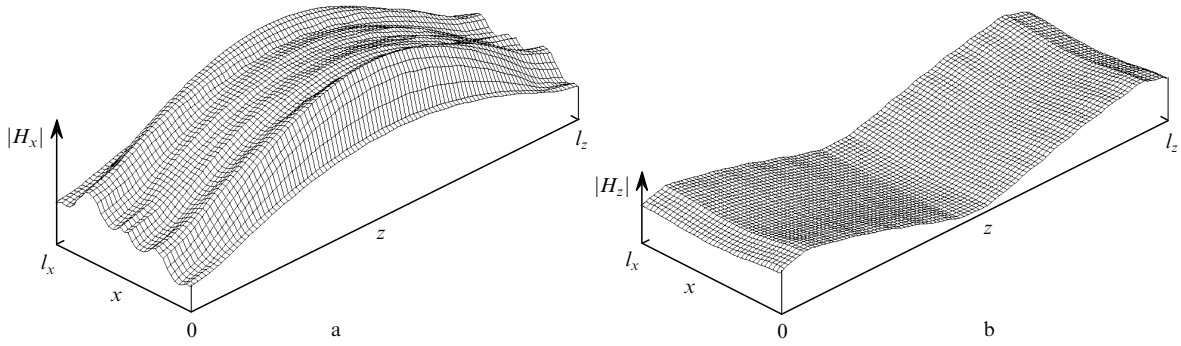

Figure 7. Spatial structure of the amplitudes of field projections $|H_x|$ (a) and $|H_z|$ (b) upon selection of the resonator fundamental mode.

fundamental mode is selected at the highest-Q Bragg resonance frequency. This mode can interpreted as an eigenmode of the two-dimensional Bragg resonator with the subscripts $\{n = 1, m = 0\}$. Thus, the highest-Q frequency and the absolute value of its Q factor found in the direct numerical simulation agree well with the analytic results. Simulation simultaneously confirms the presence of high-Q modes in the centre of the non-transparency band in the two-dimensional Bragg resonator. Note that in conventional one-dimensional Bragg structures the modes are located at the edges of the non-transparency region. In this case, there exists the problem of discrimination of a low-frequency or high-frequency mode (see, for example, [7]).

Figure 7 presents spatial field structures of partial wave fluxes under conditions of selection of the fundamental mode of the two-dimensional Bragg resonator. In fact, this figure shows distributions H_x (Fig. 7a) and H_z (Fig. 7b) of the magnetic field component. As follows from the representation for partial wave components (3), the field H_x is proportional to the sum of partial wave fluxes $|C_z^+ - C_z^-|$ propagating along the z axis and the field H_z – to the sum of fluxes $|C_x^+ - C_x^-|$ propagating along the x axis. The comparison with the analytic results (Fig. 5) shows that the field structures in the simulation reproduce with a high accuracy these results including the relation between the amplitudes of the partial waves.

Note that the resonator dimensions used above in the direct numerical simulation are not limiting from the point of view of selective possibilities and their choice is limited by the computational resources. As follows from the results of

the analytic consideration, the two-dimensional Bragg resonator preserves the selectivity upon an increase in the dimensions l_z and l_x, because, as one can see from expressions (20), (21), the relation between the mode Q factors with a different number of the field variation along the axes x and z does not depend on the above parameters. However, at a fixed coupling coefficient, the Q factors of all the modes increase and at some level will be levelled off by ohmic losses. On the other hand, a simultaneous decrease in the coupling coefficient, which can be achieved by decreasing the modulation depth of the medium, has natural technological limitations. Nevertheless, the characteristic system width l_x, at which the two-dimensional Bragg resonator ensures the mode selection, is of the order of its length l_z and the latter can have the same order as that in the case of one-dimensional resonators.

4. Conclusions

We have shown that two-dimensional doubly periodic structure (2) deposited on the dielectric surface ensures effective mode selection along two coordinates. This result has been obtained both within the framework of the method of coupled waves (geometrical optics approximation) and the direct numerical simulation. Two-dimensional Bragg structures allow one to design lasers with a two-dimensional distributed feedback. The analysis of the dynamics of these lasers within the framework of the semiclassical approach [8] has shown that at moderate excesses above the threshold it is possible to establish the stationary single-frequency lasing at large Fresnel parameters. In this case, the field distribution of partial waves in the stationary lasing regime is close to the structure of the above-described fundamental mode of the two-dimensional Bragg resonator. Note in conclusion that amplification of TM-polarised waves takes place not for all types of the active medium. For example, TM-waves are amplified in semiconductor lasers but cannot be used in heterostructure lasers. In the latter, coupling on a two-dimensional Bragg grating of TE- and TM-waves should be used. In this case, we deal with amplification of the active medium of two counterpropagating TE-modes, while TM-waves propagating in the transverse direction perform radiation mode locking of separate parts of the active medium. To this end, the description of the electrodynamic parameters of two-dimensional Bragg resonators making use of TE- and TM-wave coupling is reduced, with the accuracy to the coupling coefficient, to that presented above.

Acknowledgements. The authors thank A.A. Andronov and V.Ya. Aleshkin for useful discussions. This work was supported by Russian Foundation for Basic Research (Grant Nos 08-08-00966-a and 07-02-00617-a) and the 'Dynasty' Foundation.

References

1. Yariv A. *Quantum Electronics* (New York: Wiley, 1975).
2. Kogelnik H., Shank C.V. *J. Appl. Phys.*, **43**, 2327 (1972).
3. Kogelnik H., in *Integrated Optics* (Berlin/Heidelberg: Springer, 1979) Vol. 7.
4. Ghafouri-Shiraz H. *Distributed Feedback Laser Diodes and Optical Tunable Filters* (New York: Wiley, 2003).
5. Luk'yanov V.N., Semenov A.T., Shelkov N.V., Yakubovich S.D. *Kvantovaya Elektron.*, **2**, 2373 (1975) [*Sov. J. Quantum Electron.*, **5**, 1293 (1975)].
6. Morthier G., Baets R. *J. Lightwave Technol.*, **9**, 1305 (1991).
7. Afanas'ev A.A., Mikhnevich S.Yu. *Kvantovaya Elektron.*, **34**, 315 (2004) [*Quantum Electron.*, **34**, 315 (2004)].
8. Baryshev V.R., Ginzburg N.S., Sergeev A.S. *Pis'ma Zh. Tekh. Fiz.*, **34** (3), 47 (2008).
9. Ginzburg N.S., Peskov N.Yu., Sergeev A.S. *Opt. Commun.*, **96**, 254 (1993); *Opt. Commun.*, **112**, 151 (1994).
10. Ginzburg N.S., Peskov N.Yu., Sergeev A.S., Arzhannikov A.V., Sinitsky S.L., Phelps A.D.R., Konoplev I.V., Robb G.R.M., Cross A.W. *Phys. Rev. E*, **60**, 935 (1999).
11. Ginzburg N.S., Peskov N.Yu., Sergeev A.S., Denisov G.G., Kuzikov S.V., Zaslavsky V.Yu., Arzhannikov A.V., Kalinin P.V., Sinitsky S.L., Thumm M. *Appl. Phys. Lett.*, **92**, 103512 (2008).
12. Yablonovitch E., Gmitter T.J., Meade R.D., Rappe K., Joannopoulos J.D. *Phys. Rev. Lett.*, **67**, 3380 (1991).
13. Hirayama H., Hamano T., Aoyagi Y. *Appl. Phys. Lett.*, **96**, 791 (1996); Yoshie T., Vuckovic J., Scherer A., Chen H., Deppe D. *Appl. Phys. Lett.*, **79**, 4289 (2001).
14. Hwang J.K., Ryu H.Y., Song D.S., Han I.Y., Song H.W., Park H.G., Lee Y.H., Jang D.H. *Appl. Phys. Lett.*, **76**, 2982 (2000).